Journal of Ceramic Processing Research. Vol. 2, No. 4, pp. 160~164 (2001)

J O U R N A L
Ceramic
Processing Research

Processing and characterization of anode materials for solid oxide fuel cells

Hiroto Fukudome, Soichiro Sameshima and Yoshihiro Hirata*

Department of Applied Chemistry and Chemical Engineering, Kagoshima University, 1-21-40 Korimoto, Kagoshima [illegible] Japan

Many efforts have been devoted to the low-temperature operation of solid oxide fuel cells. Yttria-stabilized zirconia is widely used as a solid electrolyte for oxygen ions at around 1000°C. A ceria-based electrolyte may decrease the operating temperature because of its higher electrical conductivity. In this research, the processing of anode material for rare-earth-doped ceria ceramics was studied. Ni powder and Sm-doped ceria powder prepared by an oxalate coprecipitation method were mixed in different volume ratios and sintered in air at 1300°C. The sintered cermet was annealed in a mixed hydrogen-argon atmosphere for 10 h at 400°C. The electrical conductivity was measured at 25°-200°C in air for the sample before and after the annealing. Compared with the as-sintered sample, the electrical conductivity of the sample after the annealing became very high due to an increase of electronic conduction by the Ni. The electrical conductivity increased with an increase of Ni content because of the formation of a network of nickel in the matrix of Sm-doped ceria.

Key words: Sm-doped ceria, Ni, Anode, Solid oxide fuel cell, Electrical conductivity.

Introduction

It is reported that rare-earth-doped ceria has a higher oxygen ion conductivity than Y_2O_3-stabilized ZrO_2 (YSZ) and is a candidate solid electrolyte for the operation of solid oxide fuel cells (SOFCs) at low temperatures [1-9]. Reducing the operation temperature is effective for increasing the lifetime and for expanding the choice of the constituent materials such as electrodes and metal gas separators of SOFCs. The purpose of this research is to produce a high performance anode material for rare-earth-doped ceria ceramics. Some researchers have proposed the following candidate anodes: Ni/Sm-doped ceria (SDC) cermet [10], Ni/ceria-gadolinia cermet [11], Ru/SDC cermet [12], and $La_{0.9}Sr_{0.1}Ga_{0.8}Mn_{0.2}O_3$ [13]. In this experiment, Ni/SDC cermet was processed as an anode material for SDC electrolyte. The electrical properties of the cermet were analyzed in relation to its microstructure and Ni content.

Experimental Procedure

Processing of Ni/SDC composite

The detailed powder preparation method of samaria-doped ceria with a composition $Ce_{0.8}Sm_{0.2}O_{1.9}$ is reported in our previous papers [14, 15]. The starting materials were $Ce(NO_3)_3 \cdot 6H_2O$ (>98.9 mass%), $Sm(NO_3)_3 \cdot 6H_2O$ (>99.5 mass%) and $H_2C_2O_4 \cdot 2H_2O$ (>99 [illegible]). Cerium and samarium nitrate solutions of 0.2 M were mixed at the molar ratio of Ce^{3+}/Sm^{3+} = 4/1. The mixed solution was dropped into a stirred oxalic acid solution of 0.4 M to produce an oxalate coprecipitate. The precipitate was vacuum-filtered, washed with distilled water and dried at 40°C overnight. The dried oxalate coprecipitate was heated at 600°C in air to form $Ce_{0.8}Sm_{0.2}O_{1.9}$. The samaria-doped ceria powder (median size 0.87 μm) was mixed with Ni powder (99.9 [illegible], median size 10.0 μm) and compacted uniaxially under a pressure of 49 MPa to a pellet of 10 mm diameter and 2 mm thickness. The sintering of the powder compact was carried out at 1300°C for 4 h in air (DMS-6512 electric furnace, Marusho Electro-Heat Co., Ltd., Japan). The sintered cermet was annealed in a mixed hydrogen/argon (1/3, in volume ratio) atmosphere for 10 h at 400°C to reduce the NiO component to Ni metal. The phases produced in the samples before and after the annealing were identified by X-ray diffraction (Cu K_α, Model No. 2013, Rigaku Co., Japan). The bulk density of the samples was measured by the Archimedes method using distilled water. The theoretical density of SDC was calculated from the lattice parameter.

Measurement of electrical conductivity

Gold was sputtered on the surfaces of the Ni/SDC cermet before and after the annealing in a H_2/Ar atmosphere. Pt plates with lead wires were pressed and contacted to the Au electrodes. The complex impedance of the cermet in the temperature range of 25° to 200°C, was measured by a two-terminal ac [illegible]

*Corresponding author:
Tel : +81-99-285-8325
Fax: +81-99-257-4742
E-mail: eliminatehirata@apc.kagoshima-u.ac.jp

ircuit using a self-inductance-capacitance-impedance LCZ) meter (model 4276A, 4277A and 4193A, Yokogawa Hewlett-Packard Co., Japan) at 100 Hz to 10 MHz in dried air ($O_2 = 21 \pm 0.5\%$, $CO_2 \leqq 0.1$ ppm, $NO_x \leqq 0.1$ ppm, $SO_x \leqq 0.1$ ppm, dew point $\leqq 70°C$).

Results and Discussion

Density and microstructure of Ni/SDC cermet

Figure 1 shows the solid content and porosity of (a) as-sintered Ni/SDC cermet and (b) the cermet annealed in a H_2/Ar atmosphere at 400°C. The fine SDC powder was sintered in air at 1300°C to 85% theoretical density. Most of the remaining pores were open pores. The volume, size and shape of the open pores should be strictly controlled to enhance the fuel gas transport at the anode. Addition of large Ni powder to fine SDC powder caused an increase in the amount of open pores (Fig. 1(a)). In the Ni/SDC system, three kinds of particle contact are formed in the mixed powder compact: SDC-SDC, SDC-Ni, and Ni-Ni. The contact number of each depends on the fraction of Ni and the size ratio of SDC to Ni. To understand the contact numbers of particles in the Ni/SDC system, we calculated the collision frequency of colloidal particles in a solution as a first approximation. When the motion of colloidal particles is dominated by diffusion, Smoluchowski has given Eq. (1) for the number (b_{ij}) of collision per unit time for any particles in the system [16-18],

$$b_{ij} = 4\pi C_i C_j D_i r_i (r_i + r_j)\left(\frac{1}{r_i} + \frac{1}{r_j}\right) = 4\pi C_i C_j D_i r_i \left\{4 + \left[\left(\frac{r_i}{r_j}\right)^{1/2} - \left(\frac{r_j}{r_i}\right)^{1/2}\right]^2\right\} \quad (1)$$

where C_i, D_i, and r_i are the particle number concentration, diffusion coefficient and radius of the i th particle, respectively. The diffusion coefficient is inversely proportional to the radius of the particle, as indicated by Stoke's law ($D = kT/6\pi\eta r$, k : Boltzmann constant, η: viscosity). The collision frequency has a minimum at $r_i = r_j$ and becomes higher at a larger difference of particle sizes. The fractional collision frequency between particle i and j, $(FCF)_{ij}$ is defined as $b_{ij}/(b_{ii} + 2b_{ij} + b_{jj})$. Figure 2 shows the fractional collision frequency of the Ni/SDC system with $r_{Ni} = 5.0$ μm and $r_{SDC} = 0.43$ μm. The collision frequency of SDC-SDC was insensitive to the addition of Ni particles because of the large size ratio of Ni to SDC. The collision frequency of SDC-Ni increases gradually with an increase of Ni content and decreases drastically to 0 at around 100% of Ni. The coagulation of Ni-Ni particles is also accelerated with an increase of the Ni fraction and the collision frequency reaches 1 at 100% Ni. The result shown in Fig. 1(a) indicates the sinterability of the powder mixture was inhibited by the increased contact numbers of SDC-Ni and Ni-Ni. That is, the low sinterability in the contact region of SDC-Ni and Ni-Ni resulted in the formation of open pores. Therefore, a duplex structure of dense SDC-rich regions (SDC-SDC contact) and porous Ni-rich regions (Ni-SDC contact and Ni-Ni contact) is expected for the microstructure of the sintered cermet. During the sintering of the cermet in air, the Ni powder was oxidized to NiO. The density of NiO (6.96 g/cm^3) was used to calculate the solid content and porosity of the sintered cermet in Fig. 1 (a). However, the influence of this phase change on the sinterability would be small because of the large particle size of Ni and of the high phase compatibility between SDC-Ni or SDC-NiO. The microstructure and phase compatibility of the cermet is discussed latter. Annealing of the cermet in a H_2/Ar atmosphere (Fig. 1 (b)) increased the porosity of closed pores. This result is associated with the reduction of NiO to Ni. Formation of active Ni changed some open pores to closed pores by the deformation (sintering) of Ni-Ni regions.

Figure 3 shows the microstructures of the cermet sintered at 1300°C for 4 h in air. The SDC powder provided a uniform microstructure with submicrometre

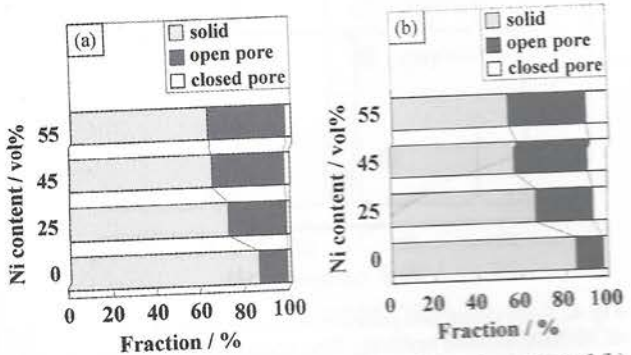

Fig. 1. Fraction of solid and pores of (a) as-sintered cermet and (b) cermet annealed in a H_2/Ar atmosphere.

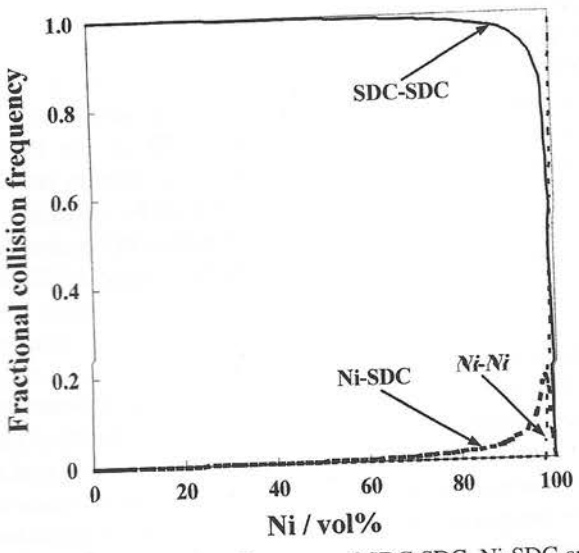

Fig. 2. Fractional collision frequency of SDC-SDC, Ni-SDC and Ni-Ni particles.

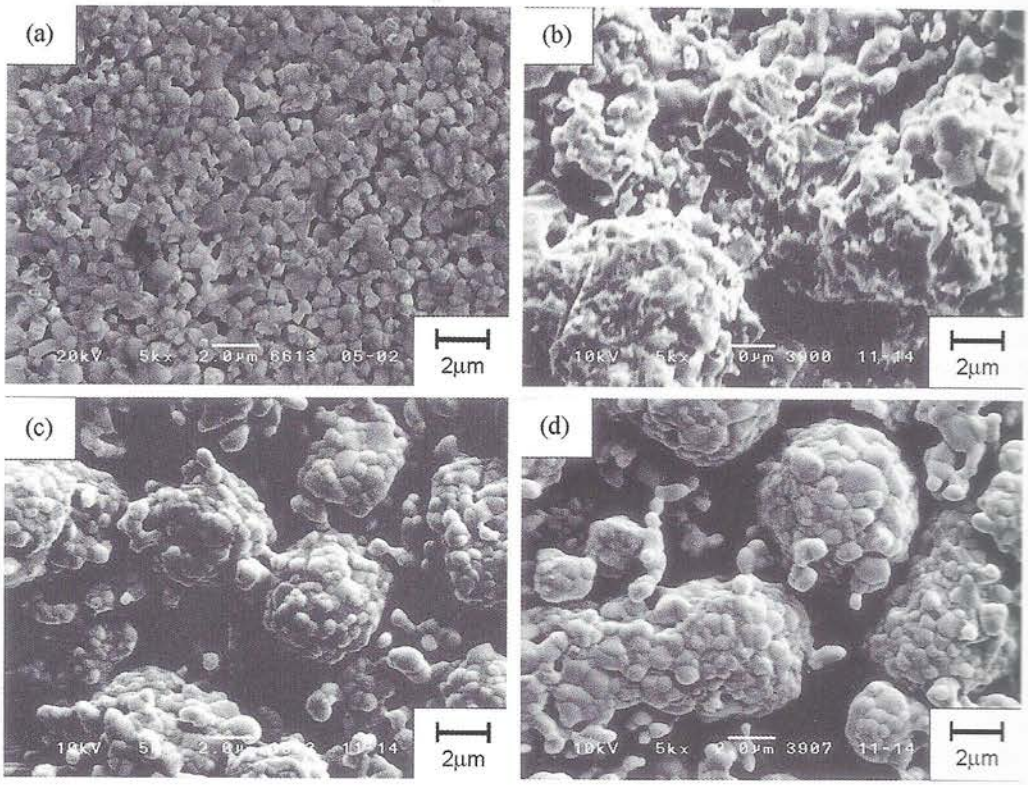

Fig. 3. Microstructures of as-sintered cermets of Ni/SDC=0/100 (a), 25/75 (b), 45/55 (c) and 55/45 vol% (d).

sized-open pores (Fig. 3(a)). Addition of 25 vol% Ni to SDC powder produced the heterogeneous microstructure (Fig. 3(b)), where the large Ni particles of about 10 μm were surrounded by fine SDC particles of about 1 μm. Further addition of Ni (Figs. 3(c), (d)) caused the isolation of SDC grains coated on the surface of Ni particles. This change in the microstructure with addition of Ni is supported by the approximate calculations illustrated in Fig. 2.

Figure 4 shows XRD patterns of SDC and Ni/SDC cermets before and after the annealing at 400°C in a H_2 /Ar atmosphere. As-sintered SDC was stable in a low oxygen pressure and no change was measured in the diffraction patterns. As seen in Fig. 4(b), NiO and SDC showed a good phase compatibility in air at 1300°C. Furthermore, NiO was reduced to Ni in the H_2/Ar atmosphere at 400°C. This annealing condition provided no interaction between Ni and SDC. The above result suggests that the Ni-SDC system can be expected to be a chemically inert system with high electronic and ionic conductivity.

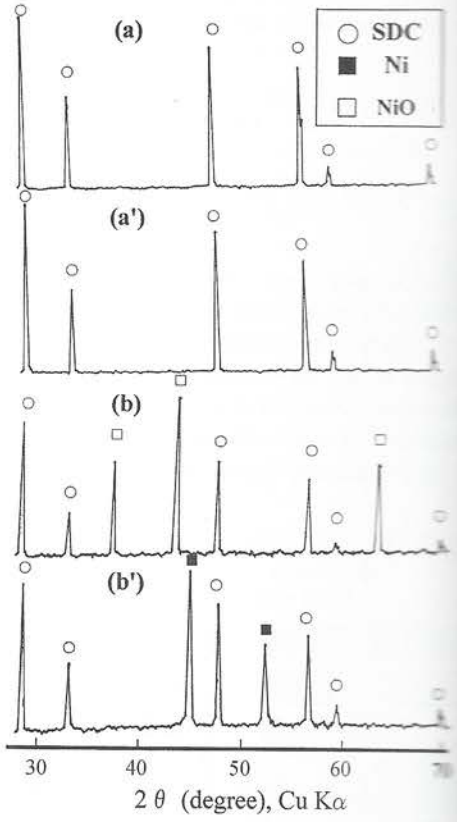

Fig. 4. X-ray diffraction patterns of as-sintered SDC (a) and cermet of Ni/SDC = 55/45 vol% (b). The phases after annealing in a H_2/Ar atmosphere at 400°C are shown in Fig. 4 (a') and (b') respectively.

Electrical conductivity of cermets

The complex impedance plots of the as-sintered Ni/SDC cermet (Ni/SDC = 45/55 vol%) are shown in Fig. 5. The impedance plots at 25° and 100°C consisted of one semicircle with the center at a negative value on the imaginary axis (Z''), suggesting a multi-relaxation mechanism of charged species. The resistance of the cermet was determined from the value of real axis (Z')

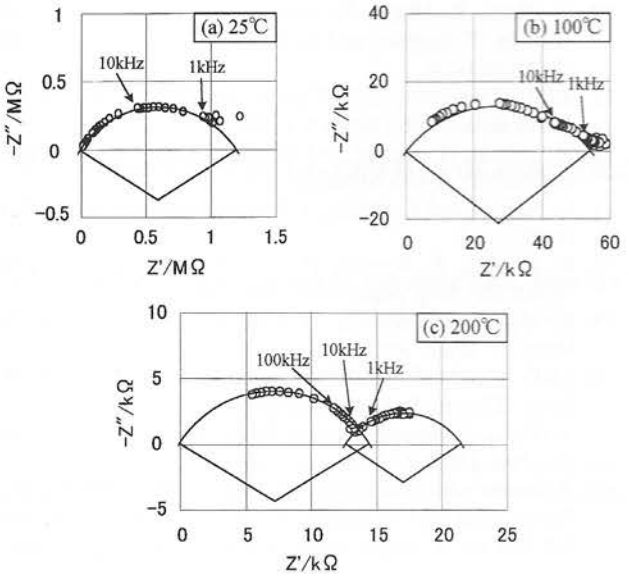

Fig. 5. Complex impedance plots of as-sintered cermet of Ni/SDC = 45/55 vol%, measured at 25°, 100° and 200°C.

at $\omega(=2\pi f$, f: frequency) $\rightarrow 0$. The impedance plot at 200°C was divided into two semicircles on the Z'-axis. The semicircle in the higher frequency range and the second semicircle in the lower frequency range may correspond to oxygen ion migration in the bulk and across the grain boundaries, respectively [19]. The electrical conductivity (σ) of the cermet was $\sigma = 2.1 \times 10^{-7}$, 4.7×10^{-6} and 1.1×10^{-5} S·cm^{-1} at 25°, 100° and 200°C, respectively. These low values are associated with (1) the low migration rate of oxygen ions at low temperatures, (2) oxidation of Ni in the as-sintered cermet and (3) interruption of the migration path of charged species by different kinds of grains. The dependence of conductivity at 200°C on the Ni content

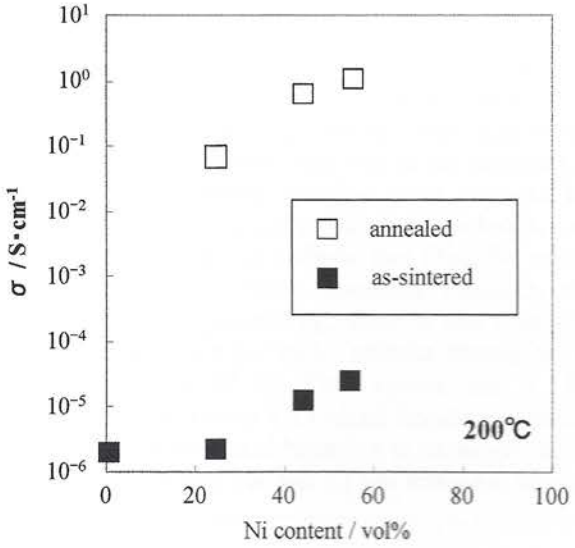

Fig. 6. Ni content dependence of electrical conductivity for as-sintered Ni/SDC cermet and the cermet annealed in a H_2/Ar atmosphere.

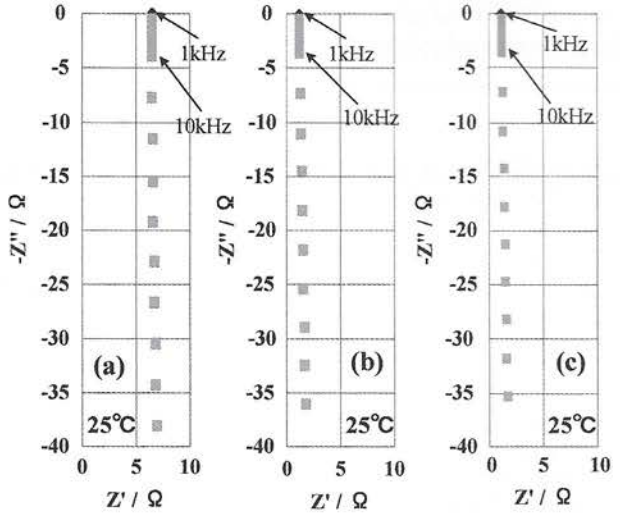

Fig. 7. Complex inpedance plots of cermets with compositions of Ni/SDC = 25/75 (a), 45/55 (b) and 55/45 vol% (c) at 25°C, after annealed in a H_2/Ar atmosphere.

is seen in Fig. 6. The conductivity showed a tendency to increase at a higher fraction of Ni. As discussed before, the increased Ni fraction enhances the contact number of NiO-NiO in the sintered cermet. The possible mechanism for the increased conductivity with Ni fraction may be the contribution of hole conduction through NiO-NiO contact. Figure 7 shows the complex impedance plots for the cermet after annealing at 400 °C in a H_2/Ar atmosphere. The shape of the impedance plot indicates the equivalent series circuit of resistance and coil (lead wire). The Z' value at $\omega \rightarrow 0$ represents the resistance of the cermet. Compared with the as-sintered cermet, a very small resistance was measured in the annealed cermet. The Ni content dependence of the conductivity is shown in Fig. 6. The conductivity of the as-sintered cermet was significantly improved by annealing in the H_2/Ar atmosphere. This result is due to the reduction of NiO to Ni. The electronic conduction of Ni dominates the conductivity. The Ni content dependence of the conductivity can be explained by the increased contact number of Ni-Ni grains.

Conclusions

Addition of large Ni powder to fine SDC powder increased the amount of open pores after sintering in air. The contact number of SDC-SDC, SDC-Ni and Ni-Ni grains in the sintered cermet depended on the fraction of Ni and the size ratio of SDC to Ni. The NiO in the as-sintered cermet was reduced to Ni by annealing in a H_2/Ar atmosphere at 400°C. A high phase compativility was observed in the SDC/NiO system and in the SDC/Ni system. The above two factors, contact number and phase compatibility, controlled the sinterability of the cermet. The electrical conductivity of as-sintered cermet was greatly improved by annealing in the H_2/Ar atmosphere. The Ni content depend-

ence of the conductivity was explained by the increased contact number of Ni-Ni grains.

References

1. H. Inaba and H. Tagawa, Solid State Ionics 83 (1996) 1-16.
2. G.M. Christie and F.P.F.V. Bekel, Solid State Ionics 83 (1996) 17-27.
3. Y. Miyazaki, Bull. Ceram. Soc. Japan 30 (1995) 322-28.
4. B.C.H. Steele, K. Zheng, R.A. Rudkin, N. Kiratzis, and M. Christie, in Proccedings of the Fourth International Symposium on Solid Oxide Fuel Cells (SOFC-IV), edited by M. Dokiya, O. Yamamoto, H. Tagawa and S.C. Singhal, (Electrochem. Soc., New Jersey, 1995) p. 1028.
5. T. Kudo and H. Obayashi, J. Electrochem. Soc. 122 (1975) 142-47.
6. H.L. Tuller and A.S. Nowick, J. Electrochem. Soc. 122 (1975) 255-59.
7. R.T. Dirstine, R.N. Blumenthal, and T.F. Kuech, J. Electrochem. Soc. 126 (1979) 264-69.
8. H. Yahiro, T. Ohuchi, K. Eguchi, and H. Arai, J. Mater. Sci. 23 (1988) 1036-41.
9. R. Gerhardt and A.S. Nowick, Solid State Ionics 5 (1981) 547-50.
10. S. Ohara, R. Maric, X. Zhang, K. Mukai, T. [illegible] Yoshida, T. Inagaki, and K. Miura, J. Power [illegible] (2000) 455-458.
11. S.J.A. Livermore, J.W. Cotton, and R.M. [illegible] Power Sources 86 (2000) 411-416.
12. H. Uchida, H. Suzuki, and M. Watanabe, J. [illegible] Soc. 145[2] (1998) 615-620.
13. C. Fanglin and L. Meilin, J. Solid State [illegible] (1998) 7-14.
14. K. Higashi, K. Sonoda, H. Ono, S. [illegible] Hirata, Key Eng. Mater. 159-160 (1999) 25-30.
15. K. Higashi, K. Sonoda, H. Ono, S. [illegible] Hirata, J. Mater. Res. 14[3] (1999) 957-67.
16. J.T.G. Overbeek, "Colloid Science I", Edited by [illegible] Kruyt (Elsevier Pub., Amsterdam 1952) p. 278.
17. Y. Hirata, N. Numaguchi, and W. H. Shih, Key Eng. [illegible] 159-160 (1999) 127-134.
18. Y. Hirata and W.H. Shih, in Proceeding of 9th [illegible] World Ceramics Congress, Ceramics: Getting [illegible] 2000's-Part B, Edited by P. Vincenzi (Techna Srl, [illegible] 1999) p. 637.
19. S. Sameshima, H. Ono, K. Higashi, K. Sonoda, Y. [illegible] and Y. Ikuma, J. Ceram. Soc. Japan 108[12] ([illegible] 1064.